



HAL
open science

Removal of organic micropollutants from domestic wastewater: The effect of ozone-based advanced oxidation process on nanofiltration

Z. Amadou Yacouba, Mendret Julie, Geoffroy Lesage, François Zaviska, S. Brosillon

► To cite this version:

Z. Amadou Yacouba, Mendret Julie, Geoffroy Lesage, François Zaviska, S. Brosillon. Removal of organic micropollutants from domestic wastewater: The effect of ozone-based advanced oxidation process on nanofiltration. *Journal of Water Process Engineering*, 2021, 39, pp.101869 -. 10.1016/j.jwpe.2020.101869 . hal-03493609

HAL Id: hal-03493609

<https://hal.science/hal-03493609v1>

Submitted on 2 Jan 2023

HAL is a multi-disciplinary open access archive for the deposit and dissemination of scientific research documents, whether they are published or not. The documents may come from teaching and research institutions in France or abroad, or from public or private research centers.

L'archive ouverte pluridisciplinaire **HAL**, est destinée au dépôt et à la diffusion de documents scientifiques de niveau recherche, publiés ou non, émanant des établissements d'enseignement et de recherche français ou étrangers, des laboratoires publics ou privés.



Distributed under a Creative Commons Attribution - NonCommercial 4.0 International License

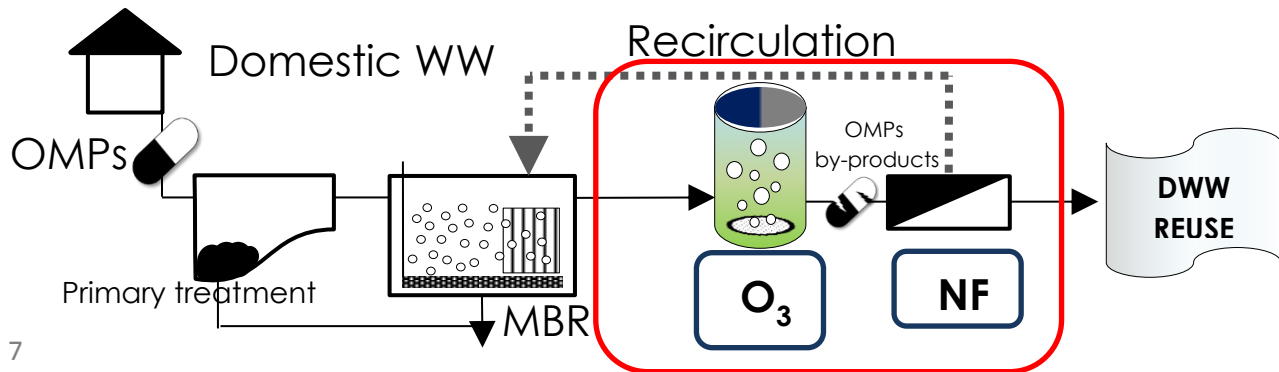
1 **Removal of organic micropollutants from domestic wastewater: the effect**
2 **of ozone-based advanced oxidation process on nanofiltration.**

3 **Z. Amadou Yacouba*, J. Mendret*, G. Lesage*, F. Zaviska*, S. Brosillon***

4 * Institut Européen des Membranes, IEM, Univ Montpellier, CNRS, ENSCM, Montpellier,

5

6 **Graphical abstract**



7

8 **Abstract**

9 The objective of this study was to develop an innovative and advanced integrated “membrane
10 and oxidation” system for the treatment of domestic wastewater by coupling membrane
11 bioreactor (MBR), nanofiltration (NF) and ozonation. Five contaminants were selected
12 (acetaminophen, carbamazepin, sulfamethoxazole, tetracyclin and terbutryn). The MBR
13 effluent samples have been fully characterized using conventional analysis (COD, TOC,
14 UV254, ionic chromatography...) and advanced characterization analyses (3D fluorescence
15 excitation–emission matrices (3DEEM)) before being spiked with 1ppm of each of the
16 selected pharmaceuticals. NF process experiments were carried out in batch and semi-batch
17 mode using a flat sheet membrane system (NF-90). Selected OMPs were well rejected by NF
18 (between 84% and 98%) and the main fouling mechanisms observed were pore blocking and
19 gel layer formation. MBR effluent was then pre-treated in an ozonation pilot unit’s with
20 ozone gas inlet fixed at 5g.Nm⁻³.The complete degradation by ozonation of carbamazepine
21 and sulfamethoxazole took 15 to 20 min and more than 30 min for terbutryn.
22 Acetaminophen, tetracyclin and dissolved organic matter were almost totally ozonated in 5
23 min. The overall mineralization rate was low. The pre-ozonation enables the NF fouling
24 resistance to be decreased by almost 40%.

25 **Keywords:** Wastewater reuse, Organic micropollutants, Nanofiltration, pre-Ozonation

26 **List of symbol**

- 27 $[O_3]_{\text{gas}}$: applied gas ozone concentration (gO_3/Nm^3)
28 ACT: acetaminophen
29 CBZ: carbamazepin
30 COD: chemical oxygen demand (gO_2/m^3)
31 Da: Dalton
32 DCOM: dissolved and colloidal organic matter
33 DWW: domestic wastewater
34 HPLC: high performance liquid chromatography
35 LC-MS/MS: liquid chromatography tandem mass spectrometry
36 MBR: membrane bioreactor
37 MWCO: molecular weight cut-off
38 NF: Nanofiltration
39 OMPs: organic micropollutants
40 RO: reverse osmosis
41 SUL: sulfamethoxazole
42 TER: terbutryn
43 TET: tetracyclin
44 TMP: transmembrane pressure (bar)
45 TOC: total organic carbon
46 TSS : Total Suspended Solid (mg/L)
47 UPW: ultrapure water
48 UV_{254} : ultra-violet absorbance at 254 nm
49 v : tangential velocity (m/s)
50 V_{reactor} : volume of reactor (m^3)
51 v_{stir} : stirring velocity (m/s)
52 WWTP : wastewater treatment plant
53 Y: permeate recovery rate (%)

54 **1. Introduction**

55 To overcome water shortage which is becoming a growing worldwide challenge, domestic
56 wastewater (DWW) must be considered as a promising water resource instead of mere waste.
57 Indeed, wastewater can be reused for different applications among which agricultural,
58 industrial and municipal uses but also for ground water recharge (Kellis et al. 2013). Even
59 though, occurrence of organic micropollutants (OMPs) in municipal wastewater constitutes an
60 important limiting factor pointed out by many authors (Bollmann et al. 2014; Dong et al.
61 2016; Gogoi et al. 2018). According to Ganiyu et al., most of the pharmaceuticals
62 administered for both human and animal uses are excreted unmodified via urine and feces and
63 directly introduced into sewage systems (Ganiyu et al. 2015). An important factor limiting the
64 wastewater reuse is the inefficiency of conventional waste water treatment plant (WWTP) in

65 removing OMPs (Martin Ruel et al. 2010). Even in the case of secondary treatment processes
66 improved by MBR, OMPs are not fully removed and some specific compounds showed really
67 low removal efficiencies (between 8 and 32% for pesticides such as atrazine and fenoprop)
68 (Ahmed et al. 2017). Consequently, pharmaceuticals and antibiotics have been found
69 widespread in different environmental compartments due to their persistence and low
70 biodegradability (Terzić et al. 2008).

71 To fulfill public regulations requirements and achieve sustainable development goals in terms
72 of ensuring safe and sustainable access to water (SDG 6, UN) (Costanza, Fioramonti, and
73 Kubiszewski 2016), tertiary treatment processes capable of removing bio-resistant compounds
74 are being developed and investigated. Activated carbon adsorption, ozonation and membrane
75 separation processes, such as NF and RO, have been investigated in wastewater treatment
76 schemes. Tight nanofiltration and reverse osmosis remove well the majority of organic
77 micropollutants (above 95%). The efficiency of such membrane processes depends mainly on
78 the type of membrane, the effluent matrix and the micropollutants physico-chemical
79 properties (Cartagena et al. 2013; Garcia-Ivars et al. 2017, Licona et al. 2018). These last
80 years, some authors have demonstrated that nanofiltration (NF) could be a good alternative to
81 reverse osmosis (RO) for urban wastewater reuse (Yangali-Quintanilla et al. 2010; Bellona et
82 al. 2012; Azaïs et al. 2017). Indeed, it offers a very good compromise between permeability
83 and selectivity. Due to the more important permeate flux compared to RO while having an
84 acceptable OMPs removal, nanofiltration requires less energy and seems more appropriate in
85 an economical point of view for the treatment of such refractory effluents (Nikbakht Fini,
86 Madsen, and Muff 2019; Song, Lee, and Ng 2020). However, there is still the problem of the
87 brine management and the propensity to fouling which both represent an object for many
88 researchers mobilization (Contreras, Kim, and Li 2009; Gan et al. 2019). Lan *et al.* have
89 investigated the performances of NF on MBR effluent and pointed out that colloidal organic
90 fouling played a major role in flux decline (Lan et al. 2018). Moreover, According to Mänttari
91 *et al.* (2000), the humic-like substances adsorb onto the polyamide-based thin film composite
92 and cellulose acetate NF membrane surface forming a gel layer which induces an additional
93 resistance to the flux passage (Mänttari et al. 2000; Azaïs et al. 2014; 2016a). Fersi *et al.*
94 distinguished two stages in fouling related to gel layer in filtration process: the gel layer
95 formation and the gel layer compression (Fersi, Gzara, and Dhahbi 2009). Because of a
96 decrease in porosity, the second stage accelerates the flux decline and this phenomenon was
97 observed after 60% of recovery rate.

118
119
120
121
122
123
124
125

Beside the membrane processes, advanced oxidation processes are also investigated for OMPs elimination (Deng 2020). They offer the advantages in degrading well micropollutants (Mizuno et al. 2018). Ozone is the second most powerful oxidizing agent after hydroxyl radicals and is much more stable than hydroxyl radicals. Ozonation was firstly used as final treatment process for effluent disinfection and to oxidize iron and manganese in the end of 19th century (Langlais, Reckhow, and Brink 2019). Nowadays, ozonation is subject to many investigation as promising treatment process to eliminate emerging OMPs (Esplugas et al. 2007; Mizuno et al. 2018; Azaïs et al. 2017). However, oxidation sometimes leads to more toxic byproducts than parent compounds and an additional treatment must be added to remove this new toxicity from the final effluent (Le et al. 2016; 2017; Oropesa et al. 2017). The aim of this study was to combine pre-ozonation and NF processes to eliminate selected OMPs in real MBR secondary effluent. Combining ozonation with NF seems an appropriate synergetic solution to take advantages of these processes while limiting their drawbacks (Byun, Taurozzi, and Tarabara 2015; Vatankhah et al. 2018; Ghernaout 2020). Indeed, while NF membrane act as an efficient physical barrier against toxicity due to OMPs and their by-products, pre-ozonation can efficiently degrades these refractory pollutants and also maintain the good flux performances of the NF process by limiting membrane fouling. The specific objectives were to investigate the fouling propensity and OMPs removal mechanisms in NF, to study the effect of the matrix composition on ozonation process and to evaluate the effect of pre-ozonation on fouling and flux evolution in NF.

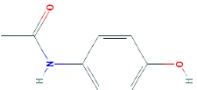
2. Materials and methods

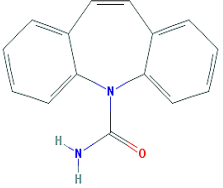
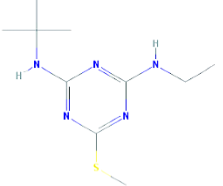
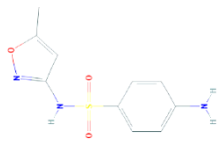
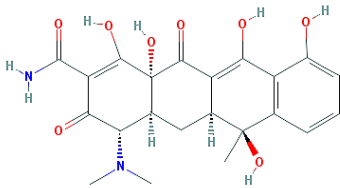
2.1 Micropollutants and matrix selection

2.1.1 Selection of micropollutants

Four pharmaceuticals, acetaminophen (ACT), carbamazepine (CBZ), sulfamethoxazole (SUL) and tetracyclin (TET) and one herbicide, terbutryn (TER) have been selected for this study.

Table 1 : Physico-chemical characteristics of selected micropollutants.

Compounds	MW g.mol ⁻¹	kO ₃ mol.l ⁻¹ .S ⁻¹	Log- K _{ow}	Charge at pH7	semi-structural formula
Acetaminophen (ACT) C ₈ H ₉ NO ₂	151	6.5 .10 ⁶ ^a	0.45	neutral	

Carbamazepin (CBZ) $C_{15}H_{12}N_2O$	236	$3.0 \cdot 10^{5b}$	2.45	neutral	
Terbutryn (TER) $C_{10}H_{19}N_5S$	241	-	3.50	neutral	
Sulfamethoxazole (SUL) $C_{10}H_{11}N_3O_3S$	253	$2.5 \cdot 10^{6b}$	0.89	negative	
Tetracyclin (TET) $C_{22}H_{24}N_2O_8$	444	$1.9 \cdot 10^{6c}$	-1.37	neutral	

126 a. (Hamdi El Najjar et al. 2014) b. (Huber et al. 2003) c. (Khan, Bae, and Jung 2010)

127 These molecules were selected because of their representativeness for different class of
 128 emerging contaminants found widespread in WWTP secondary effluent (Terzić et al. 2008;
 129 Leung et al. 2012; Nguyen et al. 2013; Yang et al. 2017; Barbosa et al. 2016), the diversity of
 130 their MW, hydrophobicity ($\text{Log } K_{ow}$) and oxidation rates (kO_3). Some of these molecules
 131 especially the terbutryn, are in the list of the 15 new priority substances which have to be
 132 completely removed from all treated WW by 2020 (DIRECTIVE 2013/39/EU). In order to be
 133 able to determine low concentrations in permeate when high rejection rate of the membrane
 134 are achieved, the feed solution was spiked with $1000 \mu\text{gL}^{-1}$ of each OMP. All the products
 135 were purchased from Sigma-Aldrich France, and were of analytical grade.

136 2.1.2 Synthetic effluent

137 As reference matrix, ultrapure water was spiked with $1000 \mu\text{gL}^{-1}$ of each targeted
 138 micropollutants. Before running any experiment with the real MBR effluent, this matrix was
 139 used first and served as comparison baseline.

140 2.1.3 Real effluent

141 The real effluent was taken from a full scale domestic WWTP equipped with MBR, located
 142 close to Montpellier, France. The plant was designed to treat $13,000 \text{ m}^3/\text{d}$ of domestic
 143 wastewater and was performing biological nitrogen removal (nitrification/denitrification).

144 MBR was equipped with KUBOTA Submerged Membrane Unit (SMU RW400) (KUBOTA,
 145 Japan) flat sheet microporous membranes made of chlorinated polyethylene (total surface of
 146 16,240 m²), with an average pore size of 0.2 μm. The characteristics of the MBR permeate are
 147 presented in Table 2. The effluent was immediately stored at nearly 4°C after sampling in
 148 order to limit the variation of the composition and rewarm at room temperature (20°C ± 1°C)
 149 before conducting the experiments. No significant change was observed in the sample
 150 characteristics after the storage period.

151 Table 2: Characteristics of real MBR effluent.

Parameters	unit	Average	Minimum	Maximum
pH		7.40	7.10	7.80
Electric conductivity	μS/cm	3300	2460	3940
TOC	mgC /L	6.70	5.50	8.60
COD	mg O ₂ /L	19.10	13.60	23.00
Absorbance at 254 nm	cm ⁻¹	0.14	0.13	0.16
SUVA ₂₅₄	L/mg/m	2.1	1.9	2.4
TSS	mg /L	2.50	2.30	2.70
Ammonium NH ₄ ⁺	mg /L	2.00	0.12	4.10
Bromure Br ⁻	mg /L	1.20	0.95	1.50
Calcium Ca ²⁺	mg /L	134.70	100.70	156.00
Chloride Cl ⁻	mg /L	602.10	498.40	754.00
Magnesium Mg ²⁺	mg /L	48.50	33.20	67.00
Nitrate NO ₃ ⁻	mg /L	9.00	3.00	30.20
Nitrate NO ₂ ⁻	mg /L	7.70	0.08	8.00
Orthophosphate PO ₄ ³⁻	mg /L	10.00	7.94	12.00
Potassium K ⁺	mg /L	34.10	22.50	44.00
Sodium Na ⁺	mg /L	321.90	287.00	370.60
Sulfate SO ₄ ²⁻	mg /L	153.70	144.50	559.50

152 2.2 Membranes selection and nanofiltration protocol

153 2.2.1 Membranes selection and characterization

154 The NF-90 polyamide membrane from DOW Filmtec has been selected for this study. This
 155 membrane is considered as a “tight” NF membrane with an estimated MWCO around 150 Da
 156 which seems appropriate for the retention of the selected micropollutant. Before
 157 experimentation, each membrane has been firstly soaked in ultrapure water to remove
 158 preservative agent then compacted at 18 bars for one hour at least or still stability of the flux
 159 was reached. Thereafter, these membranes have been fully characterized in terms of
 160 permeability and sodium chloride retention.

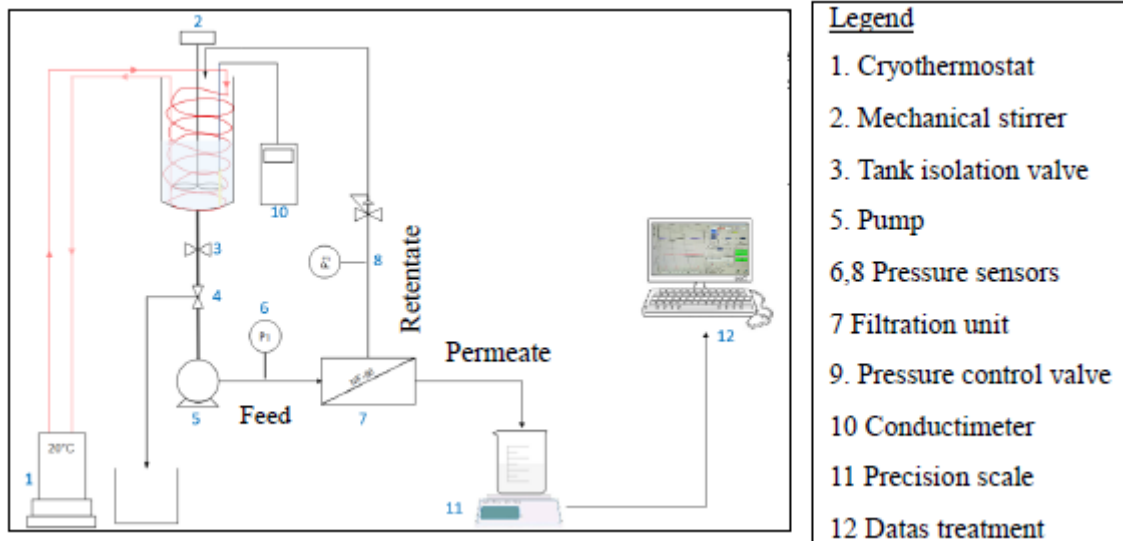
161 The NF-90 membrane permeability was determined at 10 bars at $8.4 \pm 1.0 \text{ L h}^{-1} \text{ m}^{-2} \text{ bar}^{-1}$ with
162 a NaCl rejection close to $88 \pm 4 \%$. After experiments, membranes were stored in a 200 mg L^{-1}
163 Na_2SO_3 solution at 4°C .

164 2.2.2 Cross-flow nanofiltration unit and experimental protocol

165 An Osmonics Sepa CF II cell (Sterlitech Corp.) was used to carry out the filtration
166 experiments using flat sheet membrane coupons with an effective membrane area of 140 cm^2 .
167 A pump (Hydra-Cell, Wanner Engineering, Inc.) was used to feed the Sepa cell with the
168 solution from a 16 L feed vessel. A cryothermostat (F32, Julabo) maintained constant the feed
169 water temperature ($20 \pm 1^\circ\text{C}$) to prevent an increase in liquid flow temperature. During this
170 study, the transmembrane pressure (TMP) was regulated using a micrometric pressure control
171 valve located on the retentate outlet. Experiments were performed at a cross-flow velocity
172 (v_T) of 0.5 m s^{-1} with a spacer in feed channel of 47 Mil (1.194 mm). The bench-scale NF
173 system was operated at a constant TMP of 10 bars all along the filtration experiment until
174 reaching 80% of water recovery (or at least the maximum water recovery reachable). The
175 effect of the pressure on the NF membrane efficiency has been examined at different water
176 recovery rates corresponding to ~0%, 15%, 40% and 60% at 6, 8 and 10 bar pressure. It has to
177 be noted that in order to evaluate the effect of the pressure at a fixed water recovery, the
178 concentrate and permeate was both recirculated into the feed tank.

179 Finally, after each filtration experiment the NF unit was cleaned by first recirculating caustic
180 soda (NaOH, 2%) solution then acid (HNO_3 , 2%) solution. After each base and acid cleaning,
181 the system is fully rinsed with deionized water until a conductivity of $50 \mu\text{S cm}^{-1}$ and a
182 neutral pH were reached.

183 Before the experiment, the feed water was placed in the storage tank and recirculated for 24 h
184 ($v_T = 0.5 \text{ m s}^{-1}$) without TMP to ensure that compound adsorption onto pipes and membrane
185 had reached a steady-state. The flux was recording all along the experiment by measuring the
186 permeate weight every 30 second using a scale connected to a computer. Samples were
187 collected from each compartment (feed, concentrated and permeate) for analysis. The volume
188 of the collected sample for different analysis was considered in the mass balance and the
189 apparent rejection calculation. Considering that the NF system is made of stainless steel
190 material, it was assumed that compound (micropollutant or organic matter) adsorption is
191 exclusively occurring on membrane material.



- Legend**
1. Cryothermostat
 2. Mechanical stirrer
 3. Tank isolation valve
 5. Pump
 - 6,8 Pressure sensors
 - 7 Filtration unit
 9. Pressure control valve
 - 10 Conductimeter
 - 11 Precision scale
 - 12 Datas treatment

192
193 Figure 1: Experimental setup of nanofiltration bench scale pilot.

194 2.2.3 Fouling characterization

195 Membrane fouling was estimated considering the flux recovery after different type of washing
 196 procedure. Reversible fouling was evaluated first (immediately after experiments) by
 197 conducting ultrapure water cleaning. Then, the irreversible organic fouling was evaluated by
 198 the determination of flux recovery after 6h of sodium hydroxide (0.1N) cleaning. Finally, the
 199 inorganic fouling (scaling) was determined after 6h recirculation of hydrochloride acid (0.1N)
 200 cleaning solution. The flux recovery is given by the following equation:.

201

$$Flux_{recovery} = \frac{J_{initial} - J_{cleaning}}{J_{initial} - J_{final}} \quad \text{Equation 1}$$

203

204 With:

205 $J_{initial}$: initial flux measured before the experiment (LMH)

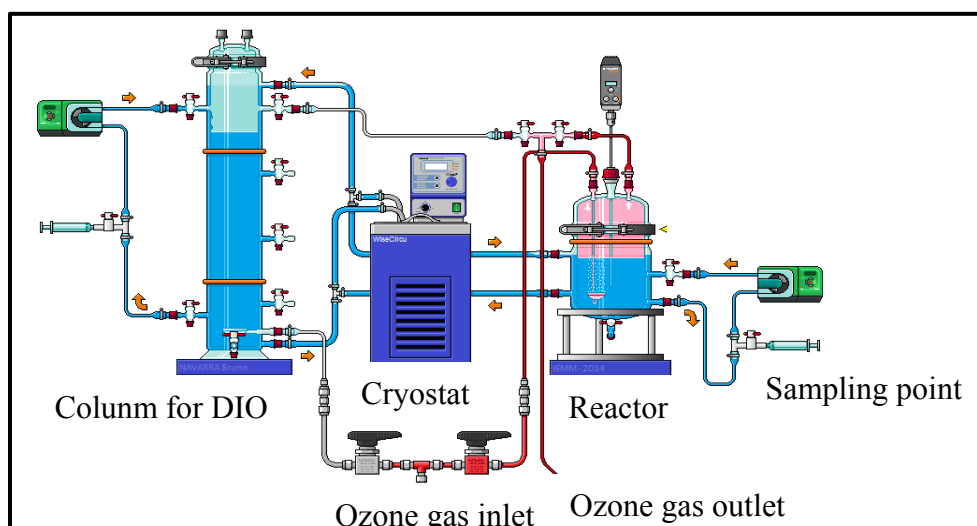
206 $J_{cleaning}$: flux measured after different cleaning steps (LMH)

207 J_{final} : final flux measured after the experiment and before the cleaning (LMH)

208 2.3 Ozone pilot semi-batch ozonation protocol

209 The ozonation lab-scale pilot consists of a glass stirred batch reactor ($V_{reactor} = 3 \text{ L}$) under
 210 thermostatic control (20°C) continuously feed by an ozone generator (BMT 803 N) from a

211 lab-grade pure oxygen tank. Before diffusion in the reactor, the ozone is diluted with the
212 oxygen to achieve a gas flow of 60 L h^{-1} and introduced from the bottom of the reactor
213 through a porous diffuser. An ozone gas analyzer (BMT 964) is used to monitor the gas ozone
214 concentration ($[\text{O}_3]_{\text{gas,in}}$) after dehumidification. The effect of pre-ozonation on NF process is
215 studied for two different reaction contact times (15 and 30 min) for which indigo method
216 (Bader and Hoigné 1981) was used to determine the dissolved ozone concentration.
217 Two electro valves connected to a computer are used to determine the desired concentration
218 for the mix oxygen/ozone. During the reaction an agitator is used to homogenized (400 rpm)
219 and increase the ozone dissolution rate in the solution. A recirculating pump is used for
220 sampling. The experiment consists in applying an ozone gas concentration and to determine
221 the transferred ozone doze. Finally the specific ozone doze was defined on a well
222 characterized effluent. Different contact times were tested depending on the parameter the
223 experiment aimed to monitor (0 min to 5 hours).



224
225 Figure 2: experimental setup of ozonation lab-scale pilot.

226 2.4 Evaluation of the nanofiltration (NF) and Ozonation systems performance

227 2.4.1 Micropollutant analysis by direct LC-MS/MS

228 Liquid chromatography-tandem mass spectrometry (LC-MS/MS) were used to quantify
229 OMPs and was performed with a Waters 2695 pump, autosampler with a $20 \mu\text{L}$ loop, a Waters
230 2695 separation module (HPLC), and a Waters Micromass (Wythenshawe, Manchester, UK)
231 Quattro Micro mass spectrometer equipped with ESI in positive mode. A C18 column (HSS-
232 T3 (100 mm * 2.1 mm, $3.5 \mu\text{m}$)) was used with eluent A (90 % HPLC grade water + 10 %
233 HPLC grade acetonitrile (ACN) + 0.1% formic acid) and eluent B (ACN + 0.1% formic acid).
234 The flow-rate was 0.25 mL min^{-1} and the injection volume was fixed at $5 \mu\text{L}$. To achieve the

235 best sensitivity, the MS was adjusted to facilitate the ionization process and the detection
 236 conditions were: capillary potential 3.5 kV, cone voltage 25 V, source temperature 120°C,
 237 desolvation temperature 450°C, cone gas flow 50 NL h⁻¹, and desolvation gas flow of 450 NL
 238 h⁻¹. Nitrogen was used as a nebulizer gas and argon as a collision gas. The collision energy
 239 was optimized for each compound (between 14 to 22 V according to the compounds). Each
 240 calibration curves were made in the same matrices as the analyte samples to avoid matrix
 241 effects on detection (external calibration). Two calibration curves were made, by analyzing
 242 standard samples before and after analyte samples, to avoid instrumental drift. Each sample
 243 was analyzed in duplicate. The instrument quantification limit (IQL) and the instrument
 244 detection limit (IDL) were determined according to a detection limit method based on a signal
 245 to noise of 3 and 10 for five replicates. The IQL and IDL obtained in ultrapure water are
 246 presented in Table 3.

247 Table 3: The instrument detection limit (IDL) and quantification limit (IQL) of selected
 248 micropollutants analysis in HPLC-MS/MS.

	IDL (µg/L)	IQL (µg/L)
ACT	4.00	11.00
CBZ	3.00	10.00
TER	22.00	65.00
SUL	0.13	0.74
TET	0.40	2.09

249

250 2.4.2 Global indicator for pollution monitoring : TOC, UV254 and SUVA analysis

251 The specific UV absorbance (SUVA₂₅₄) corresponds to the ratio of UV254 absorbance,
 252 measured in a 1 cm quartz cuvette using a UV-vis spectrophotometer (UV-2401PC,
 253 Shimadzu, Japan) and TOC value (Weishaar et al. 2003). TOC analysis was performed using
 254 a TOC-VCSN Shimadzu analyzer (Shimadzu Japan).

255 2.4.3 NF Removal rate determination

256 The NF removal rate of any parameter is determined by the difference between the feed and
 257 permeate concentrations. It is then divided by feed concentration and expressed in percentage:

$$R = \frac{C_{feed} - C_p}{C_{feed}} \quad \text{Equation 2}$$

260 With:

261 R : removal rate (%)
262 C_{feed} : concentration in feed stream
263 C_p : concentration in permeate stream

264 2.4.4 Dissolved organic matter (DOM) characterization using 3DEEM fluorescence

265 A Perkin-Elmer LS-55 spectrometer (USA) was used to produce 3DEEM spectra.
266 Measurements set-up and data analysis were described in details in Jacquin et al. (Jacquin et
267 al. 2017). Samples were scanned in ranges of 200–500 nm and 280–600 nm in excitation (Ex)
268 and emission (Em) respectively at the speed of 1500 nm/min and the increment at 10 nm,
269 while slit width was fixed at 10 nm in excitation and emission. The 3DEEM spectra were
270 divided into five fractions: Region I+ II corresponded to aromatic protein-like fluorophores
271 (tyrosine) ranging from Ex = 200–250 nm/Em m = 280–380 nm, Region III was associated
272 tfulvic acid-like fluorophores (Ex = 200–250 nm/Em m = 380–600 nm), Region IV and V
273 corresponded to proteins main derived from soluble microbial product fluorophores
274 (tryptophane) (Ex = 250–350 nm/Em m = 280–380 nm) anhumic acid-like fluorophores and
275 their hydrolysates (Ex = 380–600 nm/Em m = 250–500 nm), respective (Jacquin et al. 2018;
276 2017; Chen et al. 2003). A MilliQ water control spectra was used to normalize all spectra.

277 3. Results and discussions

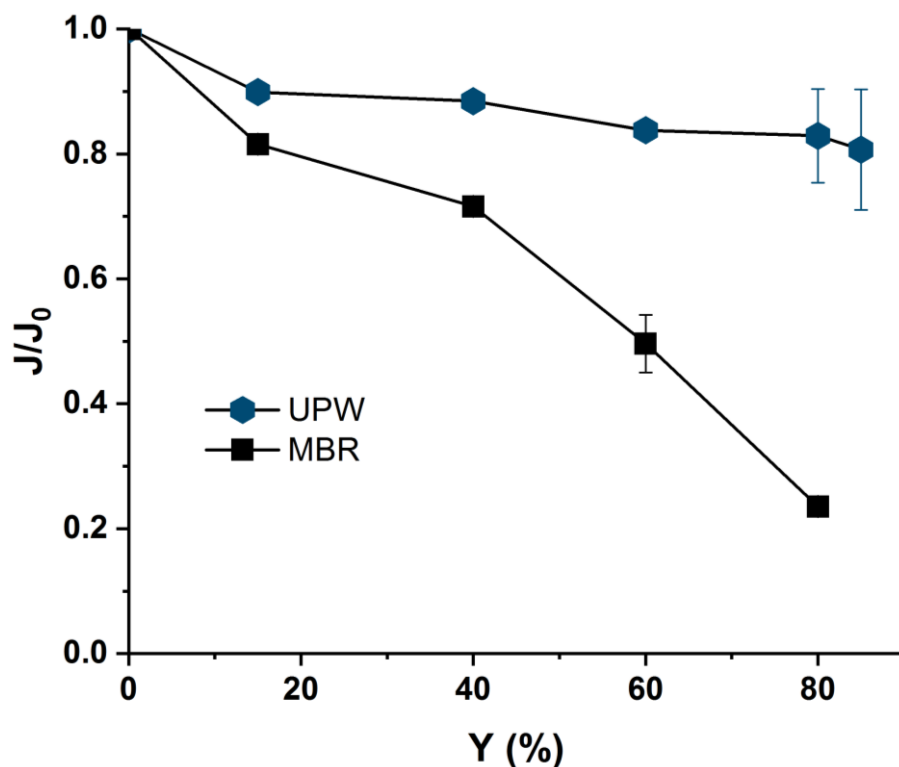
278 3.1 Performances of NF system

279 The performances of the NF system has been evaluated on both synthetic and real effluents
280 taking into account the permeate flux and OMPs retention. The experimentations have been
281 conducted during 15-25 hours in order to reach at least 80 % of water recovery ($Y=80\%$).
282 Removal rates of TOC and ions in real MBR effluent have been presented in a previous study
283 (Azais et al. 2014). Depending of the stage of fouling by real MBR effluent (with virgin
284 membrane or with fouled membranes), NF-90 membranes are able to reject between 92% and
285 98% of TOC, between 83% and 97% of monovalent ions (Cl^- , Na^+ , K^+ and NO_3^-) and between
286 93% and 100% of divalent ions (SO_4^{2-} , Mg^{2+} , Ca^{2+}).

287 3.1.1 Flux evolution

288 As a reference baseline, an experiment was conducted on ultrapure water spiked with 1000
289 $\mu\text{g/L}$ of each selected OMPS. Thereafter, same experiment was conducted (with a new
290 membrane coupon) on real MBR effluent also spiked with OMPS in order to evaluate the

291 impact of such matrix on water flux decline. The results of these experiments are presented in
 292 Figure 3 with the relative flux (ratio between the actual flux and the initial flux) on the y-axis
 293 according to the recovery rates on the x-axis:



294
 295 Figure 3: Relative flux evolution for real MBR effluent (MBR eff) and ultra-pure water
 296 (UPW): $TMP = 10$ bars, $pH = 7$, $V = 0.5 \text{ m.s}^{-1}$, $J_{0,MBR} = 53 \text{ LMH}$, $J_{0,UPW} = 63 \text{ LMH}$, $Y =$
 297 0.1% ; 15% ; 40% ; 60% , 80% and 85% .

298 The flux decline evolution associated to the filtration of the synthetic solution (the reference
 299 baseline) displays only a slight decrease in the flux, 24 % after 17 hours corresponding of
 300 85% water recovery. This might be explained by steric hindrance of higher MW OMPs and
 301 adsorption of the most hydrophobic OMPS which reduce slightly the flux. Concerning the
 302 real MBR effluent filtration, the flux decrease is much more pronounced up to 68% reduction
 303 of the initial flux after 25 hours experiment corresponding to 80% of water recovery. The
 304 major factor leading to the flux drop could come from dissolved and colloidal organic matter
 305 (DCOM) fouling associated to high molecular weight compounds such as protein-like, fulvic
 306 and humic-like substances. Such substances have been identified as revealed by the 3DEEM
 307 fluorescence spectrometry (Figure 7).

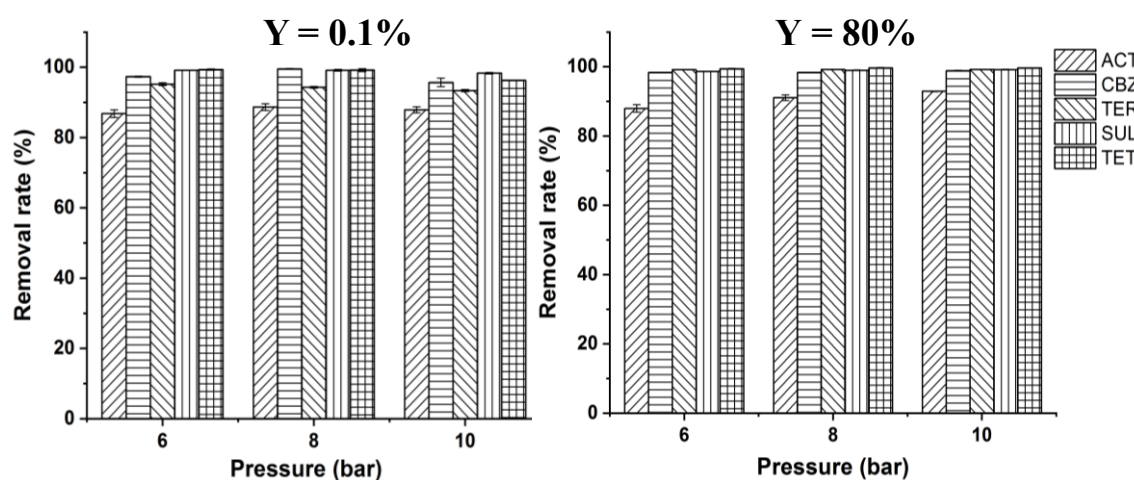
308 In addition to the colloidal fouling, the real MBR effluent contains non negligible salts
 309 concentration (see Table 2). Considering that tight NF membrane such as NF-90 has relatively
 310 high salt rejection, it induces inevitably a difference of salt concentration on both side of the

311 membrane resulting in a decrease of the driving force due to osmotic pressure difference. Salt
312 concentration increase in the feed compartment with the water recovery resulting in an
313 increasing osmotic pressure.

314 3.1.2 Monitoring of removal performances during NF: OMPs removal mechanisms

315 During the previous experiment, samples were taken from NF feed and permeate streams to
316 monitor the influence of recovery rate on selected micropollutants removal. Moreover, to
317 assess the impact of the TMP on micropollutants removal, samples were also picked for each
318 recovery rate at different pressures (6, 8 and 10 bars). Removal rates at 0.1 and 80% recovery
319 rates are shown in Figure 4.

320



321

322 Figure 4: Micropollutants removal efficiency from real MBR effluent using NF-90, TMP = 10
323 bars, $v = 0.5 \text{ m}\cdot\text{s}^{-1}$, $Y = 0.1\%$ and 80% .

324 Removal rate of micropollutants is related to its molecular weight. The bigger it is, the better
325 the removal is. Except for ACT for which the molecular weight (151 Da) is on the limit of the
326 MWCO of the membrane (estimated to 150-200 Da), a very good removal rate has been
327 observed for all the other selected micropollutants. So the main removal mechanism seems to
328 be steric hindrance as it was also observed by other authors (Garcia-Ivars et al. 2017). These
329 authors noticed an impact of real effluent matrix on the retention of uncharged
330 micropollutants. In our study, additionally to the size exclusion, an adsorption competition
331 test using calcium revealed that the tetracyclin was also adsorbed on the effluent organic
332 matter and that adsorption on organic matter may improve its retention. For the most
333 hydrophobic compounds (Carbamazepin and Terbutryn), interactions with fouled membrane
334 surface might contribute to their removal (Ganiyu et al. 2015). Sulfamethoxazol is charged

335 negatively and might undergo in electrostatic repulsive interactions with the membrane
336 surface. Thus, electrostatic repulsion could contribute to enhance its removal.

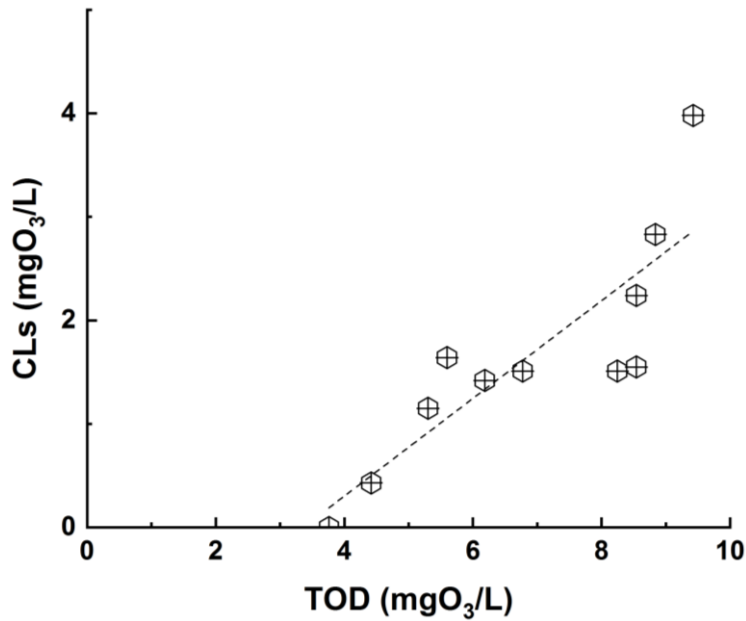
337 As shown on Figure 4, OMPs removal rate is also linked to the fouling state of the membrane.
338 OMPs removal is lower at 0.1% water recovery where the membrane was unfouled than for
339 the fouled membrane at 80% water recovery. As already observed by other authors, fouling
340 layer constitutes a second barrier to improve the NF membrane removal ability (Azaïs et al.
341 2014; Azaïs et al. 2016a; Lan et al. 2018).

342 3.2 Ozonation of MBR real effluent

343 The ozone-based degradation of dissolved organic matter (DOM) and selected
344 micropollutants was investigated and in this aim, the instantaneous ozone demand (IOD)
345 constitutes a key parameter which was first determined.

346 3.2.1 Instantaneous ozone demand determination

347 In order to optimize the specific ozone dose to apply, the IOD and consumption
348 coefficient (k) were firstly determined. The IOD corresponds to the transferred ozone dose
349 (TOD) that is instantaneously consumed by the organic matter of the effluent, with k (mn-1)
350 the consumption kinetics, before any remaining ozone is detected in the outlet liquid phase.
351 The two parameters were determined according to Roustan et al. method and their values are
352 3.76 mgO₃ / mgDOC (Figure 5) corresponding to a specific ozone doze of 0.56 mgO₃/mgC
353 and 0.064 mn⁻¹ respectively (Roustan et al. 1998).

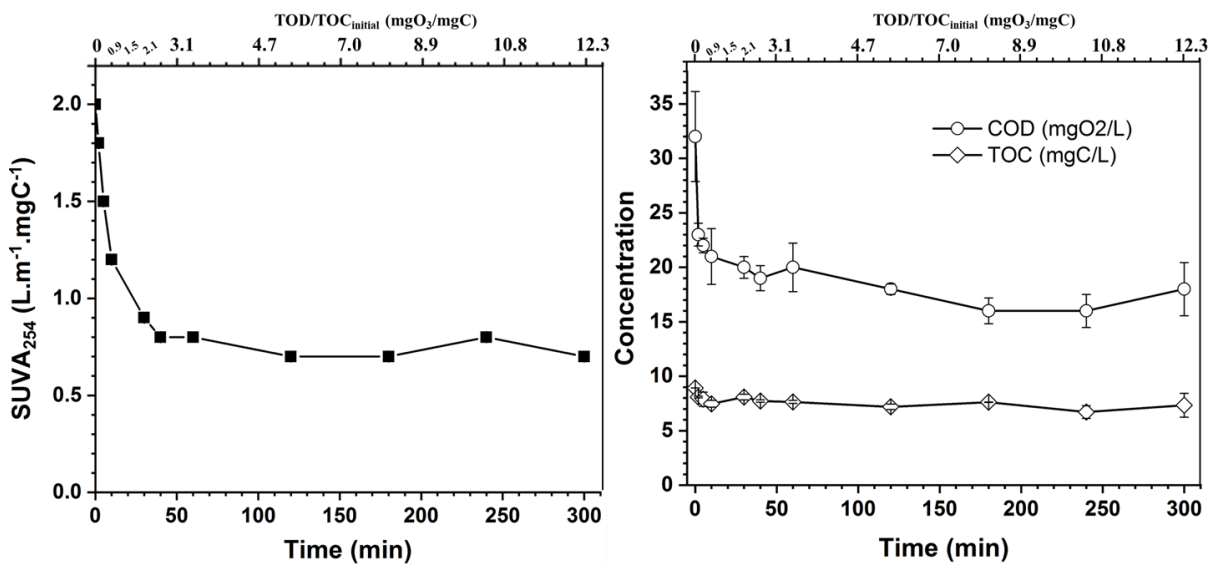


354

355 Figure 5: Determination of the instantaneous ozone demand (DIO) with: x-axis : transferred
 356 ozone doze and y-axis : dissolved ozone in the outlet liquid phase quantified by indigo-
 357 method. $V_{\text{reactor}} = 4\text{L}$, liquid flow rate = $6.7 \cdot 10^{-2} \text{ m}^3/\text{s}$. contact-time = 10 min.

358 3.2.2 Ozonation of real wastewater

359 The ozonation of the real wastewater were monitored through following parameters: UV_{254} ,
 360 COD and TOC. In order to better understand the phenomenon, the experiments were run for 5
 361 hours, Figure 6 shows the evolution of sub mentioned parameters as a function of both time
 362 and ratio TOD/TOC:



363

364 Figure 6: Evolution of global parameter of the real matrix during ozonation. left: $SUVA_{254}$,
 365 right: COD and TOC removal, $T^\circ = 20^\circ \text{C}$, $V_{\text{reactor}} = 3 \text{ L}$, $V_{\text{stir}} = 400 \text{ rpm}$, $[O_3]_{\text{gas}} = 5 \text{ gO}_3/\text{Nm}^3$.

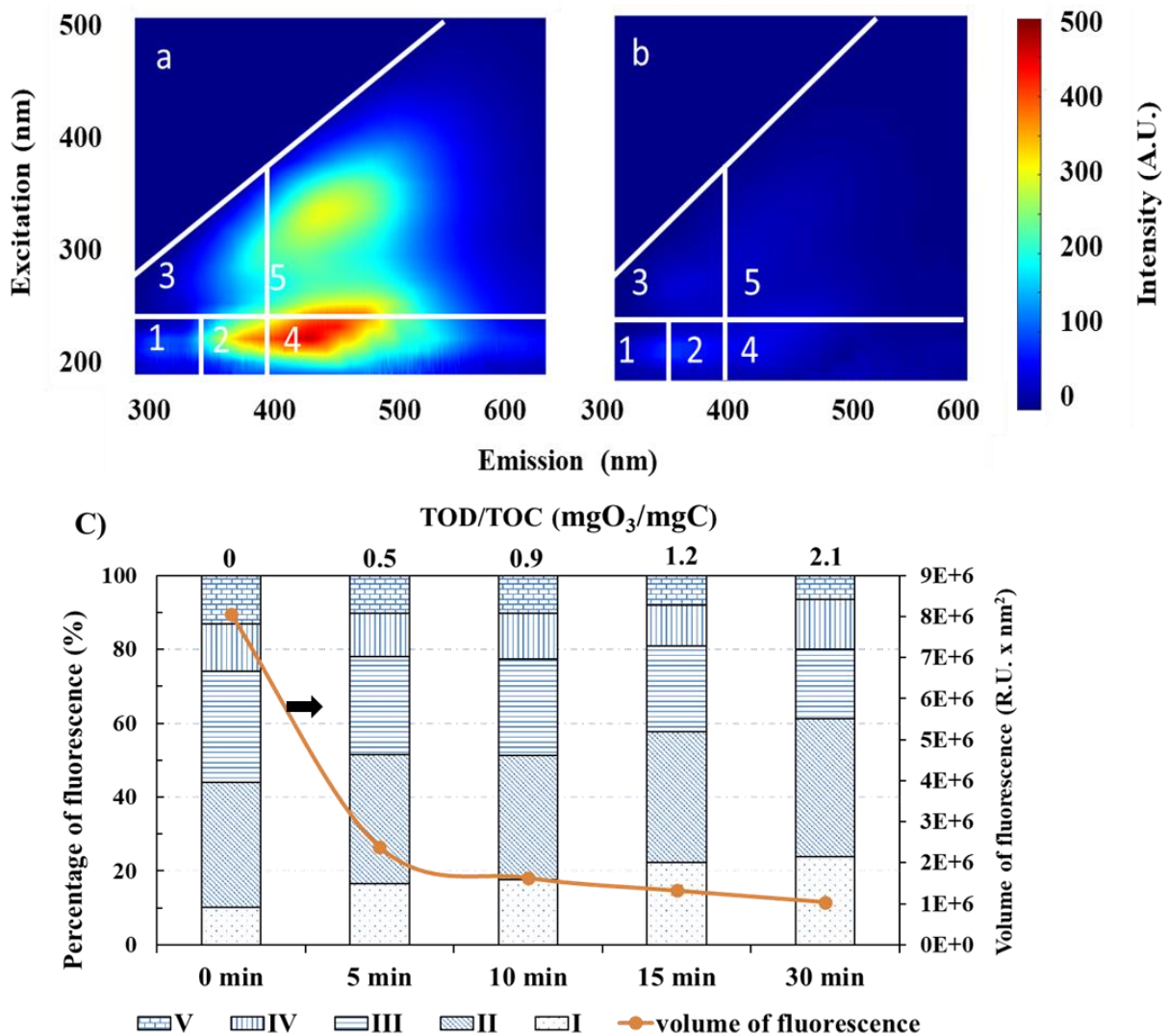
366 It can be seen in Figure 6 that the specific UV absorbance at 254 nm drastically decreases
367 since the beginning of the reaction to stabilize after 30 min (2.1 mgO₃/mgC). Indeed, by
368 attacking the double-bound of the carbon chain monitored throughout the UV absorbance at
369 254nm, the ozonation process is known to be efficient in aromaticity degradation (Azaïs et al.
370 2017; Cheng et al. 2016).

371 Moreover, the COD decreases for 40% from its initial value of 32 mgO₂ /L in the first 15 min
372 to 20 min (1.2 to 1.5 mgO₃/mgC) to stabilize around 50%.

373 As revealed by previous studies (Byun, Taurozzi, and Tarabara 2015; Azaïs et al. 2016b), the
374 curve of TOC degradation over time, confirms the inefficiency of ozone in terms of organic
375 matter mineralization, with only a very slight decrease even after five hours of ozonation
376 (Byun, Taurozzi, and Tarabara 2015). The low change in TOC is not detrimental, because
377 ozonation main goal is to limit the fouling of NF by transforming DCOM into lower MW
378 compounds. The second goal of ozone at this stage is to transform bio-refractory molecules
379 into more biodegradable compounds that should be further biodegraded (after recirculation of
380 NF concentrate to the MBR).

381 Furthermore, the evolution of organic matter was characterized through three dimensional
382 emission-excitation fluorescence (3DEEM). 3DEEM spectra and the percentage of fractions
383 are illustrated in Figure 7.

384
385



386

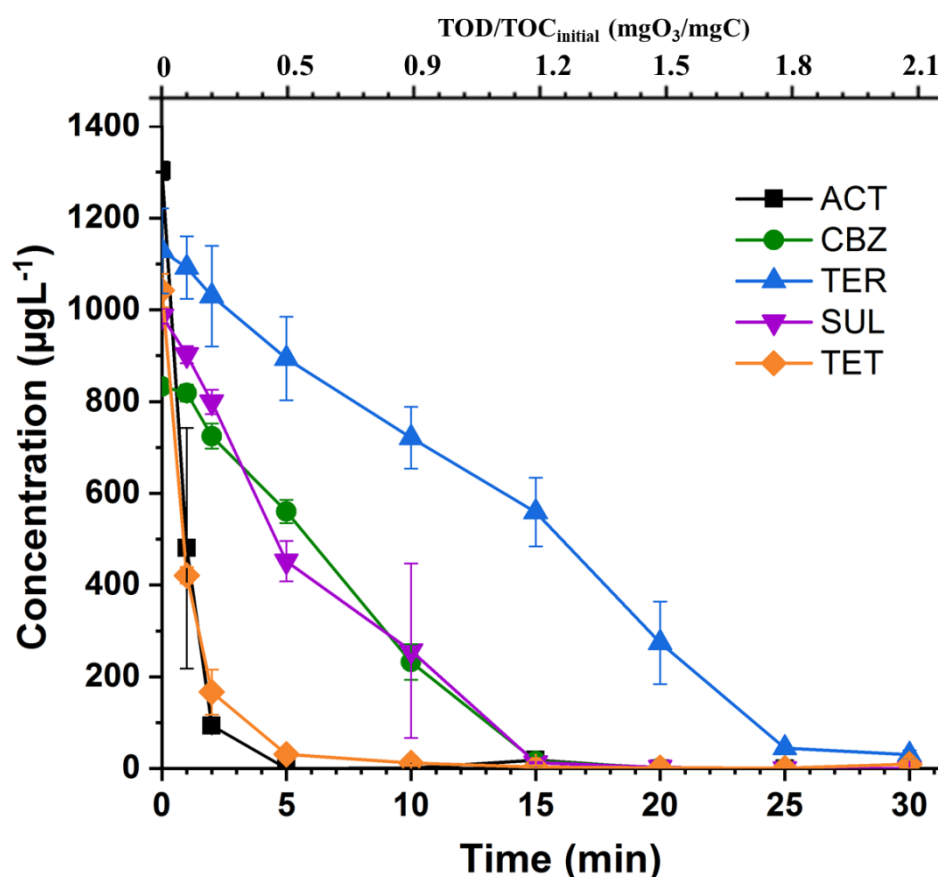
387 Figure 7: 3DEEM fluorescence spectra and volumes of fluorescence for different fractions of
 388 DCOM during ozonation ($T^{\circ} = 20^{\circ}\text{C}$, $V_{\text{reactor}} = 3\text{ L}$, $V_{\text{stir}} = 400\text{ rpm}$, $[\text{O}_3]_{\text{gas}} = 5\text{ gO}_3/\text{Nm}^3$). a)
 389 3DEEM spectra after 0 min of ozonation; b) 3DEEM spectra after 30 min of ozonation; c)
 390 volume and % volume of the five 3DEEM regions. Region I, region II, region III, region IV
 391 and region V correspond to aromatic proteins-like type I, aromatic proteins-like type II,
 392 fulvic-like, SMP-like and humic-like fluorophores, respectively.

393 3DEEM spectrum presented in Figure 7.a. demonstrate that MBR permeate is mainly
 394 constituted of fluorescent molecules located in the protein-like and SMP-like regions (zones II
 395 and III), as well as in the fulvic-like and humic-like substances regions (zones IV and V).
 396 Figure 7c shows that DOM repartition in fractions does not change significantly during 30
 397 min ozonation time (2.1 mgO₃/mgC). However, an important decrease of the overall volume
 398 of fluorescence was observed after only 5 min ozonation contact time with almost 70% drop,
 399 then a slight linearly decrease over time to reach almost 90 % drop after 30min of ozonation
 400 (Figure 7.b.). The differences between Figure 7.a. and Figure 7.b. is due to the first 5 min of
 401 reaction (0.5 mgO₃/mgC). These results are concordant with the observation of Liu *et al.* who

402 monitored the evolution of DCOM during ozonation and noticed a significant decrease in the
 403 intensities of all DCOM fluorophores after 30 min ozonation contact time (2.1 mgO₃/mgC)
 404 (Liu et al. 2016).

405 3.2.3 Ozonation of micropollutants in real wastewater

406 During the ozonation of real MBR effluent before coupling with NF, the degradation rate of
 407 five selected micropollutants has been monitored for 30 min and the results are presented in
 408 Figure 8.



409
 410 Figure 8: Evolution of OMPs concentration in doped real MBR effluent in function of time of
 411 ozonation. $V_{\text{reactor}} = 3 \text{ L}$, $V_{\text{stir}} = 400 \text{ rpm}$, $[\text{O}_3]_{\text{gas}} = 5 \text{ gO}_3/\text{Nm}^3$.

412 The monitoring of the degradation of the selected micropollutants revealed three categories of
 413 micropollutants: the first group constituted by ACT and TET which shows 90% degradation
 414 rate in the first 5 min (0.5 mgO₃/mgC) and total degradation after 10 min (0.9 mgO₃/mgC) of
 415 ozonation reaction time. This has been confirmed by some authors who have determined the
 416 ozone reactivity kinetics constants (k_{O_3}) for these molecules (Hamdi El Najjar et al. 2014;
 417 Huber et al. 2003; Khan, Bae, and Jung 2010). For ACT, Najjar et al. obtained 2.6×10^6
 418 $\text{M}^{-1} \text{s}^{-1}$ in pure water and for TET, Khan et al., evaluated the ozone reactivity kinetics
 419 constant at $1.9 \times 10^6 \text{ M}^{-1} \text{ s}^{-1}$, (Najjar et al. 2014; Khan, Bae, and Jung 2010). The second

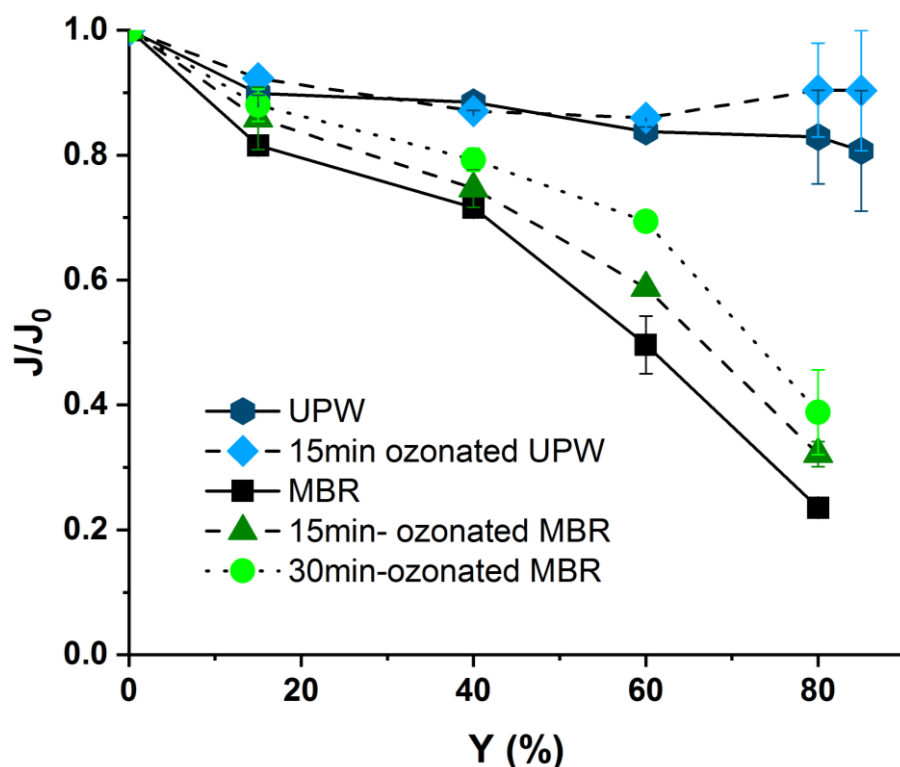
420 group composed of CBZ and SUL shows 70% degradation in the first 10 min and almost total
421 degradation after 15 min (1.2 mgO₃/mgC) to 20 min (1.5 mgO₃/mgC) of ozonation reaction
422 time. The ozone reactivity kinetics coefficients have been determined in literature for this
423 second group as well. $3.0 \times 10^5 \text{ M}^{-1} \cdot \text{s}^{-1}$ and $2.5 \times 10^6 \text{ M}^{-1} \text{ s}^{-1}$ were obtained for CBZ and
424 SUL respectively (Huber et al. 2003). Finally, the third category including TER is the less
425 reactive compound to ozone. 70% of the initial concentration is degraded by ozone after 20
426 min and only a degradation of 90% to 95% of the initial concentration is achieved after 25
427 min to 30 min (2.1 mgO₃/mgC) reaction time. Terbutryn is part of a class of micropollutants
428 (triazins) known to be more resistant to ozone degradation; the low reactivity towards ozone
429 of the compound may be explained by stability of triazinic rings (Ormad et al. 2008).

430 3.3 Impact of pre-ozonation on NF performances

431 In order to investigate the impact of the pre-ozonation on the nanofiltration performances,
432 some experiments were conducted immediately after MBR effluent ozonation. The
433 performances were compared to that of non-ozonated matrix. As the micropollutants were
434 almost totally degraded during ozonation, their removal was not monitored in ozonated matrix
435 except for the terbutryn which is still present at significant concentration (30 µg/L) but totally
436 eliminated at 80% of water recovery. So the impact of pre-ozonation on NF is limited to the
437 flux and the fouling study.

438 3.3.1 Impact of pre-ozonation on NF flux evolution

439 In this section, the impact of ozonation on nanofiltration efficiency (permeability) has been
440 studied. The flux evolution for both reference and real MBR effluent, ozonated and non-
441 ozonated, are presented in Figure 9.



443

444 Figure 9 : Monitoring of flux evolution for different ozonated matrixes spiked with
 445 micropollutants (1000 $\mu\text{g/L}$). $\text{TMP} = 10 \text{ bars}$, $v = 0.5 \text{ m}\cdot\text{s}^{-1}$. $J_{0,\text{UPW}} = 63 \text{ LMH}$, $J_{0,\text{UPW}+15\text{minO}_3} =$
 446 74 LMH , $J_{0,\text{MBR}} = 53 \text{ LMH}$, $J_{0,\text{MBR}+15\text{minO}_3} = 57 \text{ LMH}$, $J_{0,\text{MBR}+30\text{minO}_3} = 53 \text{ LMH}$. Ozonation
 447 conditions: $T^\circ = 20 \text{ }^\circ\text{C}$, $[\text{O}_3]_{\text{gas}} = 5 \text{ gO}_3/\text{Nm}^3$, ozone contact time = 15 min and 30 min
 448 corresponding to 1.2 and 2.1 mgO_3/mgC , respectively.

449 Figure 9 reveals that due to the degradation of DOM (see 3DEEM on figure 7) during the pre-
 450 ozonation, the flux decline is always lower in case of ozonated matrix than that of non-
 451 ozonated matrix. When the real effluent matrix has been ozonated for 15 min, the flux is
 452 slightly improved and the decrease in the initial flux is about 65% ($Y=80\%$). Indeed, nearly
 453 3% and 8% of flux improvement (average) can be observed after 15min and 30min ozonation
 454 respectively. These flux improvement on real ozonated effluent can be attributed to the
 455 oxidation of the protein-like, fulvic and humic-like substances as revealed by the 3DEEM
 456 fluorescence spectrometry (figure 7). Ozonation induced a structural change in DOM by
 457 decomposing carbon-carbon double bonds and aromatic rings of humic substances (Cheng et
 458 al. 2016; Stylianou et al. 2015). Concerning UPW, no significant change of flux is observed
 459 with pre-ozonation, which is logical due to the absence of DOM. It has to be noted that the
 460 evolution of the flux in case of UPW spiked or not, indicate that the presence of
 461 micropollutants induced a drop flux of about 20% for $Y=80\%$.

462 3.4 Fouling and resistance of the NF membrane.

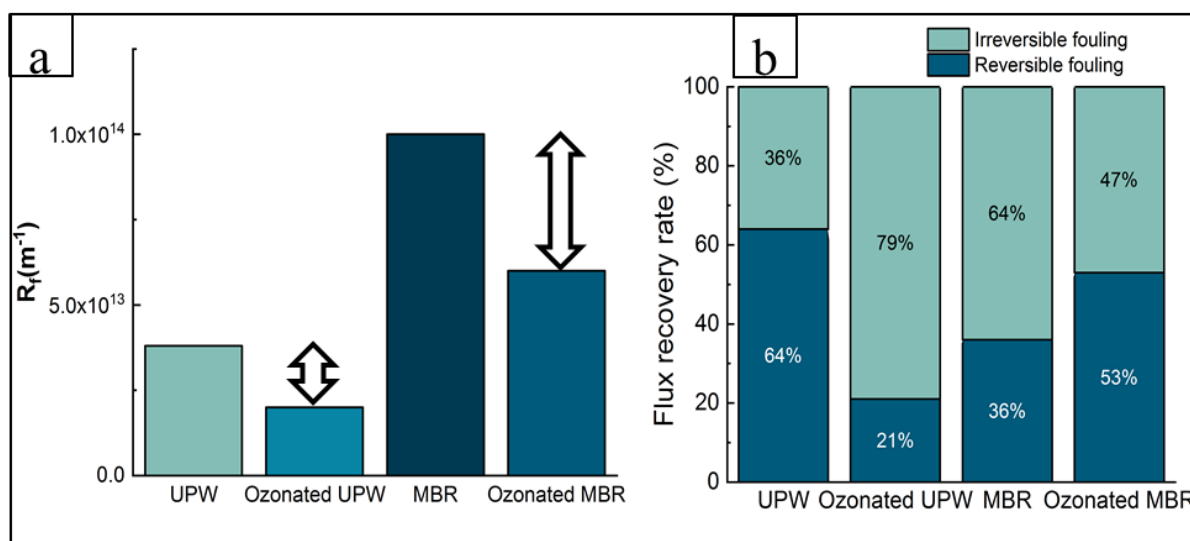
463 In order to better investigate the impact of the pre-ozonation, the resistance to the flux for
 464 both reference and real MBR effluent ozonated and non-ozonated are recapitulated in Table4.

465 Table 4: Membrane, fouling and total resistances of ozonated and non-ozonated MBR
 466 effluents and ultra pure water (UPW) after NF-90 filtrations : TMP = 10 bars, $v = 0.5 \text{ m.s}^{-1}$, $Y = 80\%$.
 467 Ozonation: $[\text{O}_3]_{\text{gas}} = 5 \text{ gO}_3/\text{Nm}^3$, ozone contact time = 15 min, $[\text{O}_3]_{\text{specific}} = 1.2$
 468 mgO_3/mgC .

Resistances ($\times 10^{13} \text{ m}^{-1}$)	UPW	Ozonated UPW	MBR	Ozonated MBR
R_m	4.06	4.00	4.04	4.08
R_f	3.63	2.33	9.99	6.51
R_{tot}	7.69	6.33	14.03	10.6

469 Table 4 revealed that the ozonation induced for both matrixes a decrease in the overall
 470 resistance. The reduction of the resistance mainly comes from fouling which was structurally
 471 modified by the ozonation as shown in Figure 10-a. Moreover, according to the type of
 472 washing and subsequent flux recovered, the percentages of reversible and irreversible fouling
 473 for reference and real MBR effluent matrixes spiked with micropollutants, ozonated and non-
 474 ozonated, were also determined and presented in Figure 10-b.

475



476
 477 Figure 10: a. Effect of ozonation on fouling and b. resistance in NF-90: TMP = 10 bars, $v =$
 478 0.5 m.s^{-1} , $Y = 80\%$. Ozonation conditions: $T^\circ = 20 \text{ }^\circ\text{C}$, $[\text{O}_3]_{\text{gas}} = 5 \text{ gO}_3/\text{Nm}^3$, ozone contact
 479 time = 15 min, $[\text{O}_3]_{\text{specific}} = 1.2 \text{ mgO}_3/\text{mgC}$.

480 Figure 10-a revealed that the pre-ozonation induced a decrease of about 40% of the fouling
 481 resistance for both matrixes. For instance, from a fouling resistance of 10^{14} m^{-1} , after
 482 ozonation of real MBR effluent, the fouling resistance is only about $6.0 \times 10^{13} \text{ m}^{-1}$. The
 483 fouling characterization confirmed that the pre-ozonation enable a mitigation of the fouling

484 propensity during NF especially in the case of real MBR effluent, by modifying the DCOM
485 structure which led to a DCOM more hydrophilic and with less propensity to promote
486 irreversible fouling (Park et al. 2017; Vatankhah et al. 2018). In fact, while for the non
487 ozonated MBR effluent only 36% of the initial flux was recovered, up to 53% of the initial
488 flux were recovered by a mere ultrapure water cleaning for membrane fouled by ozonated real
489 MBR effluent (Figure 10-b). The opposite effect was observed in the case of UPW because
490 the fouling mainly came from OMPs. After ozonation, the OMPs were degraded except the
491 terbutryn which might induce a slightly higher irreversible fouling.

492

493 **4 Conclusion**

494 The overall objective of the paper was to investigate the impact of a pre-ozonation on NF
495 process performances during tertiary treatment of a MBR secondary effluent. Fouling and
496 micropollutants removal mechanisms during nanofiltration experiments with real MBR
497 effluent have been investigated. Degradation of a mixture of five micropollutants and DOM
498 during ozonation were also studied. Fouling investigation revealed that size exclusion was
499 the main mechanism of micropollutants rejection. In addition, gel layer onto fouled
500 membrane formed a supplementary barrier which contributed to enhance micropollutants
501 retention. The micropollutants were globally well retained by NF-90 membrane.

502 During ozonation, relatively high degradation rates were achieved for micropollutants,
503 requiring different specific ozone doses. In fact, while CBZ and SUL require a specific
504 ozone dose of 1.2 mgO₃/mgC and TER require a specific ozone dose of 1.5 mgO₃/mgC to
505 be degraded, 0.5 mgO₃/mgC are sufficient for the degradation of ACT and TET. The
506 dissolved organic matter was significantly degraded as well, by ozone but the overall
507 mineralization rate was low. A forthcoming study will investigate the rejection of ozonation
508 by-products by NF-90.

509 A pre-ozonation enables the fouling resistance to be decreased by almost 40%. To sum up,
510 it was demonstrated that coupling NF to a pre-ozonation process is twicly benefic. Firstly,
511 it degrades well the micropollutants preventing from expensive specific processes in NF
512 retentates management. Secondly, it also mitigates NF fouling by degrading the DOM
513 inducing concomitantly to flux improvement a decrease in membrane cleaning frequency
514 and a subsequent improve of membrane lifetime.

515 **Acknowledgements**

516 The authors acknowledge the French National Agency for Research for supporting this
517 study through the convention ANR JCJC 2016 project SAWARE (ANR-16-CE04-0002-01).
518 They are also thankful to Eddy Petit and Loubna Karfane Atfane for the technical support.

519 **References**

- 520 Ahmed, Mohammad Boshir, John L. Zhou, Huu Hao Ngo, Wenshan Guo, Nikolaos S. Thomaidis, and
521 Jiang Xu. 2017. "Progress in the Biological and Chemical Treatment Technologies for
522 Emerging Contaminant Removal from Wastewater: A Critical Review." *Journal of Hazardous*
523 *Materials* 323 (February): 274–98. <https://doi.org/10.1016/j.jhazmat.2016.04.045>.
- 524 Azaïs, Antonin, Julie Mendret, Guillaume Cazals, Eddy Petit, and Stephan Brosillon. 2017. "Ozonation
525 as a Pretreatment Process for Nanofiltration Brines: Monitoring of Transformation Products
526 and Toxicity Evaluation." *Journal of Hazardous Materials* 338 (September): 381–93.
527 <https://doi.org/10.1016/j.jhazmat.2017.05.045>.
- 528 Azaïs, Antonin, Julie Mendret, Sana Gassara, Eddy Petit, André Deratani, and Stephan Brosillon. 2014.
529 "Nanofiltration for Wastewater Reuse: Counteractive Effects of Fouling and Matrice on the
530 Rejection of Pharmaceutical Active Compounds." *Separation and Purification Technology* 133
531 (September): 313–27. <https://doi.org/10.1016/j.seppur.2014.07.007>.
- 532 Azaïs, Antonin, Julie Mendret, Eddy Petit, and Stephan Brosillon. 2016a. "Evidence of Solute-Solute
533 Interactions and Cake Enhanced Concentration Polarization during Removal of
534 Pharmaceuticals from Urban Wastewater by Nanofiltration." *Water Research* 104
535 (Supplement C): 156–67. <https://doi.org/10.1016/j.watres.2016.08.014>.
- 536 ———. 2016b. "Influence of Volumetric Reduction Factor during Ozonation of Nanofiltration
537 Concentrates for Wastewater Reuse." *Chemosphere* 165 (December): 497–506.
538 <https://doi.org/10.1016/j.chemosphere.2016.09.071>.
- 539 Bader, H., and J. Hoigné. 1981. "Determination of Ozone in Water by the Indigo Method." *Water*
540 *Research* 15 (4): 449–456.
- 541 Barbosa, Marta O., Nuno F. F. Moreira, Ana R. Ribeiro, Manuel F. R. Pereira, and Adrián M. T. Silva.
542 2016. "Occurrence and Removal of Organic Micropollutants: An Overview of the Watch List
543 of EU Decision 2015/495." *Water Research* 94 (May): 257–79.
544 <https://doi.org/10.1016/j.watres.2016.02.047>.
- 545 Bellona, Christopher, Dean Heil, Christopher Yu, Paul Fu, and Jörg E. Drewes. 2012. "The Pros and
546 Cons of Using Nanofiltration in Lieu of Reverse Osmosis for Indirect Potable Reuse
547 Applications." *Separation and Purification Technology* 85 (February): 69–76.
548 <https://doi.org/10.1016/j.seppur.2011.09.046>.
- 549 Bollmann, Ulla E., Camilla Tang, Eva Eriksson, Karin Jönsson, Jes Vollertsen, and Kai Bester. 2014.
550 "Biocides in Urban Wastewater Treatment Plant Influent at Dry and Wet Weather:
551 Concentrations, Mass Flows and Possible Sources." *Water Research* 60 (September): 64–74.
552 <https://doi.org/10.1016/j.watres.2014.04.014>.
- 553 Byun, Seokjong, Julian S. Taurozzi, and Volodymyr V. Tarabara. 2015. "Ozonation as a Pretreatment
554 for Nanofiltration: Effect of Oxidation Pathway on the Permeate Flux." *Separation and*
555 *Purification Technology* 149 (July): 174–82. <https://doi.org/10.1016/j.seppur.2015.05.035>.
- 556 Cartagena, Pablo, Marouane El Kaddouri, Vicente Cases, Arturo Trapote, and Daniel Prats. 2013.
557 "Reduction of Emerging Micropollutants, Organic Matter, Nutrients and Salinity from Real
558 Wastewater by Combined MBR–NF/RO Treatment." *Separation and Purification Technology*
559 110 (June): 132–43. <https://doi.org/10.1016/j.seppur.2013.03.024>.
- 560 Chen, Wen, Paul Westerhoff, Jerry A. Leenheer, and Karl Booksh. 2003. "Fluorescence
561 Excitation–Emission Matrix Regional Integration to Quantify Spectra for Dissolved Organic
562 Matter." *Environmental Science & Technology* 37 (24): 5701–10.
563 <https://doi.org/10.1021/es034354c>.

564 Cheng, Xiaoxiang, Heng Liang, An Ding, Fangshu Qu, Senlin Shao, Bin Liu, Hui Wang, Daoji Wu, and
565 Guibai Li. 2016. "Effects of Pre-Ozonation on the Ultrafiltration of Different Natural Organic
566 Matter (NOM) Fractions: Membrane Fouling Mitigation, Prediction and Mechanism." *Journal*
567 *of Membrane Science* 505 (May): 15–25. <https://doi.org/10.1016/j.memsci.2016.01.022>.

568 Contreras, Alison E., Albert Kim, and Qilin Li. 2009. "Combined Fouling of Nanofiltration Membranes:
569 Mechanisms and Effect of Organic Matter." *Journal of Membrane Science* 327 (1): 87–95.
570 <https://doi.org/10.1016/j.memsci.2008.11.030>.

571 Costanza, Robert, Lorenzo Fioramonti, and Ida Kubiszewski. 2016. "The UN Sustainable Development
572 Goals and the Dynamics of Well-Being." *Frontiers in Ecology and the Environment* 14 (2): 59–
573 59. <https://doi.org/10.1002/fee.1231>.

574 Deng, Hui. 2020. "A Review on the Application of Ozonation to NF/RO Concentrate for Municipal
575 Wastewater Reclamation." *Journal of Hazardous Materials*, January, 122071.
576 <https://doi.org/10.1016/j.jhazmat.2020.122071>.

577 Dong, Huiyu, Xiangjuan Yuan, Weidong Wang, and Zhimin Qiang. 2016. "Occurrence and Removal of
578 Antibiotics in Ecological and Conventional Wastewater Treatment Processes: A Field Study." *Journal*
579 *of Environmental Management* 178 (August): 11–19.
580 <https://doi.org/10.1016/j.jenvman.2016.04.037>.

581 Esplugas, Santiago, Daniele M. Bila, Luiz Gustavo T. Krause, and Márcia Dezotti. 2007. "Ozonation and
582 Advanced Oxidation Technologies to Remove Endocrine Disrupting Chemicals (EDCs) and
583 Pharmaceuticals and Personal Care Products (PPCPs) in Water Effluents." *Journal of*
584 *Hazardous Materials, Pollution Prevention and Restoration of the Environment*, 149 (3): 631–
585 42. <https://doi.org/10.1016/j.jhazmat.2007.07.073>.

586 Fersi, Cheima, Lassaad Gzara, and Mahmoud Dhahbi. 2009. "Flux Decline Study for Textile
587 Wastewater Treatment by Membrane Processes." *Desalination* 244 (1): 321–32.
588 <https://doi.org/10.1016/j.desal.2008.04.046>.

589 Gan, Zhendong, Xing Du, Xuewu Zhu, Xiaoxiang Cheng, Guibai Li, and Heng Liang. 2019. "Role of
590 Organic Fouling Layer on the Rejection of Trace Organic Solutes by Nanofiltration:
591 Mechanisms and Implications." *Environmental Science and Pollution Research* 26 (33):
592 33827–37. <https://doi.org/10.1007/s11356-018-2478-0>.

593 Ganiyu, Soliu O., Eric D. van Hullebusch, Marc Cretin, Giovanni Esposito, and Mehmet A. Oturan.
594 2015. "Coupling of Membrane Filtration and Advanced Oxidation Processes for Removal of
595 Pharmaceutical Residues: A Critical Review." *Separation and Purification Technology* 156
596 (December): 891–914. <https://doi.org/10.1016/j.seppur.2015.09.059>.

597 Garcia-Ivars, Jorge, Lucia Martella, Manuele Massella, Carlos Carbonell-Alcaina, Maria-Isabel Alcaina-
598 Miranda, and Maria-Isabel Iborra-Clar. 2017. "Nanofiltration as Tertiary Treatment Method
599 for Removing Trace Pharmaceutically Active Compounds in Wastewater from Wastewater
600 Treatment Plants." *Water Research* 125 (November): 360–73.
601 <https://doi.org/10.1016/j.watres.2017.08.070>.

602 Ghernaout, Djamel. 2020. "On the Treatment Trains for Municipal Wastewater Reuse for Irrigation." *OALib* 07 (02): 1–15. <https://doi.org/10.4236/oalib.1106088>.

604 Gogoi, Anindita, Payal Mazumder, Vinay Kumar Tyagi, G. G. Tushara Chaminda, Alicia Kyoungjin An,
605 and Manish Kumar. 2018. "Occurrence and Fate of Emerging Contaminants in Water
606 Environment: A Review." *Groundwater for Sustainable Development* 6 (March): 169–80.
607 <https://doi.org/10.1016/j.gsd.2017.12.009>.

608 Hamdi El Najjar, Nasma, Arnaud Touffet, Marie Deborde, Romain Journal, and Nathalie Karpel Vel
609 Leitner. 2014. "Kinetics of Paracetamol Oxidation by Ozone and Hydroxyl Radicals, Formation
610 of Transformation Products and Toxicity." *Separation and Purification Technology* 136
611 (Supplement C): 137–43. <https://doi.org/10.1016/j.seppur.2014.09.004>.

612 Huber, Marc M., Silvio Canonica, Gun-Young Park, and Urs von Gunten. 2003. "Oxidation of
613 Pharmaceuticals during Ozonation and Advanced Oxidation Processes." *Environmental*
614 *Science & Technology* 37 (5): 1016–24. <https://doi.org/10.1021/es025896h>.

615 Jacquin, Céline, Geoffroy Lesage, Jacqueline Traber, Wouter Pronk, and Marc Heran. 2017. "Three-
616 Dimensional Excitation and Emission Matrix Fluorescence (3DEEM) for Quick and Pseudo-
617 Quantitative Determination of Protein- and Humic-like Substances in Full-Scale Membrane
618 Bioreactor (MBR)." *Water Research* 118 (July): 82–92.
619 <https://doi.org/10.1016/j.watres.2017.04.009>.

620 Jacquin, Céline, Benoit Teychene, Laurent Lemee, Geoffroy Lesage, and Marc Heran. 2018.
621 "Characteristics and Fouling Behaviors of Dissolved Organic Matter Fractions in a Full-Scale
622 Submerged Membrane Bioreactor for Municipal Wastewater Treatment." *Biochemical
623 Engineering Journal* 132 (April): 169–81. <https://doi.org/10.1016/j.bej.2017.12.016>.

624 Kellis, M, I. K Kalavrouziotis, and P Gikas. 2013. "Review of Wastewater Reuse in the Mediterranean
625 Countries, Focusing on Regulations and Policies for Municipal and Industrial Applications."
626 *Global NEST Journal* 15 (3): 333–50. <https://doi.org/10.30955/gnj.000936>.

627 Khan, M. Hammad, Hyokwan Bae, and Jin-Young Jung. 2010. "Tetracycline Degradation by Ozonation
628 in the Aqueous Phase: Proposed Degradation Intermediates and Pathway." *Journal of
629 Hazardous Materials* 181 (1): 659–65. <https://doi.org/10.1016/j.jhazmat.2010.05.063>.

630 Lan, Yandi, Karine Groenen-Serrano, Clémence Coetsier, and Christel Causserand. 2018.
631 "Nanofiltration Performances after Membrane Bioreactor for Hospital Wastewater
632 Treatment: Fouling Mechanisms and the Quantitative Link between Stable Fluxes and the
633 Water Matrix." *Water Research* 146 (December): 77–87.
634 <https://doi.org/10.1016/j.watres.2018.09.004>.

635 Langlais, Bruno, David A. Reckhow, and Deborah R. Brink. 2019. *Ozone in Water Treatment:
636 Application and Engineering*. Routledge.

637 Le, Thi Xuan Huong, Thi Van Nguyen, Zoukifli Amadou Yacouba, Laetitia Zoungrana, Florent Avril,
638 Duy Linh Nguyen, Eddy Petit, et al. 2017. "Correlation between Degradation Pathway and
639 Toxicity of Acetaminophen and Its By-Products by Using the Electro-Fenton Process in
640 Aqueous Media." *Chemosphere* 172 (April): 1–9.
641 <https://doi.org/10.1016/j.chemosphere.2016.12.060>.

642 Le, Thi Xuan Huong, Thi Van Nguyen, Zoukifli Amadou Yacouba, Laetitia Zoungrana, Florent Avril,
643 Eddy Petit, Julie Mendret, et al. 2016. "Toxicity Removal Assessments Related to Degradation
644 Pathways of Azo Dyes: Toward an Optimization of Electro-Fenton Treatment." *Chemosphere*
645 161 (October): 308–18. <https://doi.org/10.1016/j.chemosphere.2016.06.108>.

646 Leung, H. W., T. B. Minh, M. B. Murphy, James C. W. Lam, M. K. So, Michael Martin, Paul K. S. Lam,
647 and B. J. Richardson. 2012. "Distribution, Fate and Risk Assessment of Antibiotics in Sewage
648 Treatment Plants in Hong Kong, South China." *Environment International*, Emerging
649 Environmental Health Issues in Modern China, 42 (July): 1–9.
650 <https://doi.org/10.1016/j.envint.2011.03.004>.

651 Licona, K. P. M., Geaquinto, L. D. O., Nicolini, J. V., Figueiredo, N. G., Chiapetta, S. C., Habert, A. C., &
652 Yokoyama, L. (2018). Assessing potential of nanofiltration and reverse osmosis for removal of
653 toxic pharmaceuticals from water. *Journal of Water Process Engineering*, 25, 195-204.

654 Liu, Chen, Penghui Li, Xiangyu Tang, and Gregory V. Korshin. 2016. "Ozonation Effects on Emerging
655 Micropollutants and Effluent Organic Matter in Wastewater: Characterization Using Changes
656 of Three-Dimensional HP-SEC and EEM Fluorescence Data." *Environmental Science and
657 Pollution Research* 23 (20): 20567–79. <https://doi.org/10.1007/s11356-016-7287-8>.

658 Mänttari, Mika, Liisa Puro, Jutta Nuortila-Jokinen, and Marianne Nyström. 2000. "Fouling Effects of
659 Polysaccharides and Humic Acid in Nanofiltration." *Journal of Membrane Science* 165 (1): 1–
660 17. [https://doi.org/10.1016/S0376-7388\(99\)00215-X](https://doi.org/10.1016/S0376-7388(99)00215-X).

661 Martin Ruel, S., M. Esperanza, J.-M. Choubert, I. Valor, H. Budzinski, and M. Coquery. 2010. "On-Site
662 Evaluation of the Efficiency of Conventional and Advanced Secondary Processes for the
663 Removal of 60 Organic Micropollutants." *Water Science and Technology* 62 (12): 2970–78.
664 <https://doi.org/10.2166/wst.2010.989>.

665 Mizuno, Tadao, Fei Han, Jie Xu, Yasunari Kusuda, and Hiroshi Tsuno. 2018. "Performance Evaluation
666 of Ozonation and an Ozone/Hydrogen Peroxide Process toward Development of a New

667 Sewage Treatment Process—Focusing on Organic Compounds and Emerging Contaminants.”
668 *Ozone: Science & Engineering* 40 (5): 339–55.
669 <https://doi.org/10.1080/01919512.2018.1435110>.

670 Najjar, Nasma, Arnaud Touffet, Marie Deborde, Romain Journal, and Nathalie Leitner. 2014. “Kinetics
671 of Paracetamol Oxidation by Ozone and Hydroxyl Radicals, Formation of Transformation
672 Products and Toxicity.” *Separation and Purification Technology* 136 (November): 137–143.
673 <https://doi.org/10.1016/j.seppur.2014.09.004>.

674 Nguyen, Luong N., Faisal I. Hai, Shufan Yang, Jinguo Kang, Frederic D.L. Leusch, Felicity Roddick,
675 William E. Price, and Long D. Nghiem. 2013. “Removal of Trace Organic Contaminants by an
676 MBR Comprising a Mixed Culture of Bacteria and White-Rot Fungi.” *Bioresource Technology*
677 148 (November): 234–41. <https://doi.org/10.1016/j.biortech.2013.08.142>.

678 Nikbakht Fini, Mahdi, Henrik Tækker Madsen, and Jens Muff. 2019. “The Effect of Water Matrix, Feed
679 Concentration and Recovery on the Rejection of Pesticides Using NF/RO Membranes in
680 Water Treatment.” *Separation and Purification Technology* 215 (May): 521–27.
681 <https://doi.org/10.1016/j.seppur.2019.01.047>.

682 Ormad, M. P., N. Miguel, A. Claver, J. M. Matesanz, and J. L. Ovelleiro. 2008. “Pesticides Removal in
683 the Process of Drinking Water Production.” *Chemosphere* 71 (1): 97–106.
684 <https://doi.org/10.1016/j.chemosphere.2007.10.006>.

685 Oropesa, Ana Lourdes, Fernando Juan Beltrán, António Miguel Floro, Juan José Pérez Sagasti, and
686 Patricia Palma. 2017. “Ecotoxicological Efficiency of Advanced Ozonation Processes with TiO₂
687 and Black Light Used in the Degradation of Carbamazepine.” *Environmental Science and
688 Pollution Research*, November. <https://doi.org/10.1007/s11356-017-0602-1>.

689 Park, Minkyu, Tarun Anumol, Julien Simon, Flavia Zraick, and Shane A. Snyder. 2017. “Pre-Ozonation
690 for High Recovery of Nanofiltration (NF) Membrane System: Membrane Fouling Reduction
691 and Trace Organic Compound Attenuation.” *Journal of Membrane Science* 523 (February):
692 255–63. <https://doi.org/10.1016/j.memsci.2016.09.051>.

693 Roustan, Michel, Hunert Debellefontaine, Zdravka Do-Quang, and Jean-Pierre Duguet. 1998.
694 “Development of a Method for the Determination of Ozone Demand of a Water.” *Ozone
695 Science and Engineering* 20: 513–20.

696 Song, Weilong, Lai Yoke Lee, and How Yong Ng. 2020. “Chapter 21 - Nanofiltration and Reverse
697 Osmosis Processes for the Removal of Micro-Pollutants.” In *Current Developments in
698 Biotechnology and Bioengineering*, edited by Sunita Varjani, Ashok Pandey, R. D. Tyagi, Huu
699 Hao Ngo, and Christian Larroche, 527–52. Elsevier. <https://doi.org/10.1016/B978-0-12-819594-9.00021-8>.

701 Stylianou, S. K., S. D. Sklari, D. Zamboulis, V. T. Zaspalis, and A. I. Zouboulis. 2015. “Development of
702 Bubble-Less Ozonation and Membrane Filtration Process for the Treatment of Contaminated
703 Water.” *Journal of Membrane Science* 492: 40–47.
704 <https://doi.org/10.1016/j.memsci.2015.05.036>.

705 Terzić, Senka, Ivan Senta, Marijan Ahel, Meritxell Gros, Mira Petrović, Damia Barcelo, Jutta Müller, et
706 al. 2008. “Occurrence and Fate of Emerging Wastewater Contaminants in Western Balkan
707 Region.” *Science of The Total Environment* 399 (1): 66–77.
708 <https://doi.org/10.1016/j.scitotenv.2008.03.003>.

709 Vatankhah, Hooman, Conner C. Murray, Jacob W. Brannum, Johan Vanneste, and Christopher
710 Bellona. 2018. “Effect of Pre-Ozonation on Nanofiltration Membrane Fouling during Water
711 Reuse Applications.” *Separation and Purification Technology* 205 (October): 203–11.
712 <https://doi.org/10.1016/j.seppur.2018.03.052>.

713 Weishaar, James L., George R. Aiken, Brian A. Bergamaschi, Miranda S. Fram, Roger Fujii, and
714 Kenneth Mopper. 2003. “Evaluation of Specific Ultraviolet Absorbance as an Indicator of the
715 Chemical Composition and Reactivity of Dissolved Organic Carbon.” *Environmental Science &
716 Technology* 37 (20): 4702–8. <https://doi.org/10.1021/es030360x>.

717 Yang, Yi, Yong Sik Ok, Ki-Hyun Kim, Eilhann E. Kwon, and Yiu Fai Tsang. 2017. “Occurrences and
718 Removal of Pharmaceuticals and Personal Care Products (PPCPs) in Drinking Water and

719 Water/Sewage Treatment Plants: A Review.” *Science of The Total Environment* 596–597
720 (October): 303–20. <https://doi.org/10.1016/j.scitotenv.2017.04.102>.
721 Yangali-Quintanilla, Victor, Sung Kyu Maeng, Takahiro Fujioka, Maria Kennedy, and Gary Amy. 2010.
722 “Proposing Nanofiltration as Acceptable Barrier for Organic Contaminants in Water Reuse.”
723 *Journal of Membrane Science* 362 (1): 334–45.
724 <https://doi.org/10.1016/j.memsci.2010.06.058>.
725